Characteristics of genetically diverse Antarctic sea ice bacteriophages allow adaptation to changing environmental conditions

Tatiana A. Demina[1, 2], Anne-Mari Luhtanen[3], Simon Roux[4], and Hanna M. Oksanen[1*]

[1]Molecular and Integrative Biosciences Research Programme, Faculty of Biological and Environmental Sciences, University of Helsinki, Helsinki, Finland

[2]Department of Microbiology, Faculty of Agriculture and Forestry, University of Helsinki, Helsinki, Finland

[3]Marine Research Centre, Finnish Environment Institute, Helsinki, Finland

[4]DOE Joint Genome Institute, Lawrence Berkeley National Laboratory, Berkeley, USA

*Corresponding author, Molecular and Integrative Biosciences Research Programme, Faculty of Biological and Environmental Sciences, Viikinkaari 9, University of Helsinki, FIN-00014 University of Helsinki, Finland; Telephone number: +358 2941 59104; E-mail: hanna.oksanen@helsinki.fi

Abstract

Abstract. Despite generally appreciated significant roles of microbes in sea ice and polar waters, detailed studies of virus-host systems from such environments have been so far limited by only a few isolates. Here, we investigated infectivity under changing conditions, infection cycles, and genetic diversity of four bacteriophages isolated from Antarctic sea ice: PANV1, PANV2, OANV1, and OANV2, infecting common sea ice bacterial species *Paraglaciecola* or *Octadecabacter*. Although the phages are marine and cold-active, replicating at 0-5 °C, they all survived temporal incubations at ≥30 °C and remained infectious without any salts or supplemented only with magnesium, suggesting a robust virion assembly maintaining integrity under a wide range of conditions. Host recognition in the cold proved to be effective, and the release of progeny viruses occurred as a result of cell lysis or host growth retardation. The analysis of viral genomes showed that nearly half of the gene products of each virus are unique, highlighting that sea ice harbors unexplored virus diversity. Based on predicted genes typical for tailed dsDNA phages, we suggest placing the four studied viruses in the class *Caudoviricetes*. Searching against viral sequences from metagenomic assemblies revealed that related viruses are not restricted to Antarctica, but also found in distant marine environments, indicating possible virus movement between biotopes.

Importance. Very little is known about sea ice microbes despite the significant role of sea ice in the global oceans as well as microbial input into biogeochemical cycling. The impact of possible climatic changes on Antarctic sea ice microbial communities is also poorly understood. Studies on the sea ice viruses have been typically limited to -omics-based approaches and microscopic examinations of sea ice samples. Up to date, only four cultivable viruses have been isolated from Antarctic sea ice. Our study of these unique isolates advances the understanding of the diversity of viruses in sea ice environments, their interactions with host microbes, adaptation potential in the realm of global climate change, and possible links to other biomes. Such information contributes to more accurate future predictions on microbial feedback loops as the response to global changes.

Introduction

Sea ice covers a significant area of polar oceans every year, affecting ocean ecology, biogeochemical cycles, and climate (1, 2). Although being an extreme environment, sea ice, especially its liquid brines, is inhabited by various microorganisms, including viruses (3-7). Physical and chemical changes in sea ice, under-ice water, and atmosphere, as well as microbial activity affect the brine properties and channel network (1, 5, 8). Temperatures in the brines may vary between -35° C and 0° C, affecting the thickness of channels (8): e.g., at higher temperatures, channels are more spacious, and the brine channel network may even open to the under-ice water, flushing salts and nutrients out and thus creating significant salinity changes (9, 10). Salinity and nutrient concentrations across the brine channel network may also depend on flooding on top of the ice (5, 7) and thickness of snow cover (11-13).

Cooling of surface waters and an overall increase in sea ice extent have been observed in Antarctica over the past few decades (14, 15), masking reduced ocean mixing and rapid pervasive subsurface water warming around Antarctica caused by the release of meltwater (16). However, this increased ice cover was surprisingly warm and permeable e.g., during Antarctic mid-winter 2017 (10). Substantial freshening has also been observed in the Southern Ocean in recent decades, with possibly

major contribution from the northward freshwater transport by Antarctic sea ice (17). Other phenomena related to climate change, such as ocean acidification, are also seen in Antarctica with potential microbial feedback loops that are not yet well predicted (18). Currently, we lack systematic understanding of how varying temperatures, salinity and pH may alter the functioning of microbial communities in sea ice.

Metagenomic studies have revealed high diversity and abundance of viruses in polar aquatic environments (19-21). Virus-like particles concentrations and virus-to-bacterium ratios in sea ice are typically higher than in the surrounding seawater, suggesting active virus production in the ice (22-27). The role of viruses in controlling host abundance is significant in polar environments also due to the lower abundance and diversity of grazers (21, 28). Virus infections in sea ice are not restricted to lytic cycles, but can include lysogenic ones (28, 29) and possibly pseudolysogeny (30). Viruses may also confer properties beneficial to their host survival (31). Low temperature environments in general are suggested to be hot spots of microbial evolution (30).

The studies of sea ice viruses have been typically limited to microscopic examinations and -omics approaches, while only a few virus-host systems have been isolated from sea ice so far (31-34). Here, we used four phages isolated from Antarctic sea ice (34) to study their infectivity under varying key environmental factors, as well as infection cycles, genetic diversity, and occurrence in different environments. Better understanding the role of viruses in sea ice microbial communities would provide information to be included in future sea ice models.

Materials and Methods

Growth conditions and virus infectivity

Viruses and bacteria (Table 1) were grown aerobically at 4 or 5 °C in Zobell RC medium as previously described (34). The effect of temperature on virus infectivity was tested by incubating virus stocks at 4-55 °C for 1 h. The effects of Na^+ and Mg^{2+} ions were assessed by diluting virus stocks 1000-fold in SM buffer (50 mM Tris-HCl, pH 7.5, 100 mM NaCl, 8 mM $MgSO_4$; (32)), SM buffer lacking either NaCl or $MgSO_4$, or both, or lacking $MgSO_4$ but supplemented with 10 mM ethylenediaminetetraacetic acid (EDTA) and incubating at 4 °C for 1 and 5 h. The effect of pH was tested similarly using SM buffer either with 50 mM NaH_2PO_4 (pH 3, 5, 7.5) or Tris-HCl (pH 7.5, 9). After all incubations, virus infectivity was assessed by plaque assay as previously described (34). Single-factor ANOVA test was used when three or more groups were compared or t-Test (Two-Sample Assuming Equal Variances) when comparing two groups. Groups were considered statistically not different if $p>0.05$.

Adsorption and infection cycle

To determine adsorption efficiency and rates, exponentially growing host cultures (OD_{550}~0.8) were infected with a multiplicity of infection (MOI) of ~0.001 and incubated aerobically at 4 °C. Samples in which cells were replaced with broth were used as controls. To determine the number of unbound viruses, samples were diluted in 4 °C broth (1:10 or 1:100), cells were removed (Eppendorf table centrifuge, 16 200 g, 5 min, 4 °C), and supernatants were subjected to plaque assay. The percentage of adsorption was calculated from all (particles in broth) and unbound particles (in infected cultures)

(% bound particles $= \frac{all-unbound}{all} \times 100\%$). Adsorption rate constant was calculated as (k): $= \frac{2.3}{B \times t} \times log \frac{p0}{p}$, where B is cell concentration, $p0$ and p are free virus concentrations at time point zero and after time period t, respectively (35).

For life cycle studies, IceBac 372 (OD_{550}~0.8) was infected with PANV1 or PANV2 (MOI 10) and incubated aerobically at 5 °C. Uninfected culture was used as a control. The numbers of infective free viruses in culture supernatants (Eppendorf table centrifuge, 16 200 g, 5 min, 4 °C) were determined by plaque assay. IceBac 419 and IceBac 430 cells (OD_{550}~0.8) were collected (Eppendorf table centrifuge, 16 200 g, 5 min, 4 °C) and resuspended in OANV1 or OANV2 virus stocks, respectively, (MOI of ~8) or in broth (uninfected controls). During the growth, the numbers of free viruses and viable cells in supernatant and pellet fractions (Eppendorf table centrifuge, 16 200 g, 5 min, 4 °C) were determined by plaque assay.

Virus purification and transmission electron microscopy

OANV1 was purified from virus stocks by ammonium sulfate precipitation and rate-zonal ultracentrifugation in sucrose using SM buffer as described (34). Particles were negatively stained with uranyl acetate (2% (w/v), pH 7) or Nano-W (2% (w/v) methylamine tungstate, pH 6.8) prior transmission electron microscopy (Hitachi HT780 microscope, Electron Microscopy Unit, University of Helsinki). Particle size was measured using the ImageJ (36).

Genome sequencing and annotation

Nucleic acids were extracted from purified viruses by phenol-ether extraction, precipitated by ethanol-NaCl, sequenced using Illumina MiSeq (DNA Sequencing and Genomics core facility, Helsinki Institute of Life Science, University of Helsinki) and assembled with SPAdes version 3.9.0 (37). Sequences are available in the GenBank database (MW805361, PANV1; MW805362, PANV2; MW805363, OANV1; MW805364, OANV2).

Geneious Prime 2021.0.2 (https://www.geneious.com) was used for sequence handling. ORFs were predicted using Glimmer, GeneMarkS (Prokaryotic, v. 3.26), MetaGeneAnnotator (http://metagene.nig.ac.jp/), and FGENESV (http://www.softberry.com/berry.phtml?topic=virus&group=programs&subgroup=gfindv). GC% was calculated with Genomics %G~C Content Calculator (https://www.sciencebuddies.org/science-fair-projects/references/genomics-g-c-content-calculator). Transmembrane helices were predicted using TMHMM Server v. 2.0 (https://services.healthtech.dtu.dk/service.php?TMHMM-2.0). Whole genome comparisons for overall nucleotide identity were done with EMBOSS stretcher (38). Blastn with the whole virus genomes as queries against non-redundant (nr) nucleotide collection (viruses taxid 10239) was used for searching homologous viral genome sequences. Predicted ORFs were assigned with functions based on homology searches with blastx or blastp against nr protein database (thresholds: E-value 0.00001, query cover 30%, identity 30%) (39), blast conserved domains (E-value threshold 0.01) (40), and HHpred within the Toolkit (E-value threshold 0.01) (41) (searches dated 05.2019-02.2021). VIRFAM was used for putative virus classification based on their neck gene module organization (42). tRNA genes were predicted using tRNAscan-SE v. 2.0 (43).

Metagenomic analyses

Virus sequences were searched against Integrated Microbial Genomes/Virus (IMG/VR) database (44) using the whole genomes as queries and blastn search with the maximum E-value of 0.00001 (search dated 09.12.2020). Sequence similarities were visualized using Circoletto based on Circos (45), with blastn search E-value threshold of 0.00001. For pairwise sequence comparisons, Easyfig v. 2.2.2 was used (46).

Results

Antarctic sea ice phages tolerate elevated temperatures and lowered salinity

To assess the stability of virus infectivity at different temperatures, viruses were incubated at 4 to 55 °C, using 4 °C as a reference (100% infectivity) (Fig 1). All four viruses stayed fully infectious when temporally exposed to the temperatures up to 30-45 °C. No statistically significant difference was observed in PANV1 infectivity at 4 and 35 °C, whereas the titer dropped to ~2 % at 40 °C, and only ~0.001% of particles were infective at 45 °C. For PANV2, 45 °C temperature had no statistically significant effect on the infectivity, but a sharp titer drop to ~0.03% was observed at 50 °C. OANV1 preserved the titer at 25 °C, while at 30 and 35 °C, the infectivity was ~28% and ~7.5%, respectively. For OANV2, no statistically significant difference in titers at 4 °C and 40 °C was observed, but only ~4% of particles were infective after incubating at 45 °C. Virus titers decreased one-tenth or more at 40, 50, 35, and 45 °C for PANV1, PANV2, OANV1, and OANV2, respectively. The titers were under the detection limit ($<1\times10^3$ PFU/ml), at 50, 55, 40 and 50 °C for PANV1, PANV2, OANV1, and OANV2, respectively (Fig 1).

All viruses remained infectious without NaCl (Fig. 2 a-d, buffer 2). Moreover, PANV1 and PANV2 infectivity was preserved in the absence of both NaCl and Mg^{2+}, even if residual Mg^{2+} ions were totally removed by the chelating agent, EDTA (Fig. 2 a, b, buffers 3-5). When only $MgSO_4$ was excluded from SM buffer, OANV1 titer dropped by 4-5 orders of magnitude, and OANV2 titer dropped to one-tenth (Fig. 2 c, d, buffer 3). If removing all residual Mg^{2+} ions using EDTA (Fig. 2 c, d, buffer 4), OANV1 titer was under the detection limit ($<1\times10^4$ PFU/ml), and OANV2 titer dropped 100-fold. When both NaCl and $MgSO_4$ were removed (Fig. 2 c, d, buffer 5), OANV1 and OANV2 titers were $<1\times10^4$ PFU/ml.

No statistically significant difference in virus titers was observed when virus stocks were incubated in SM buffer pH 7.5 either with Tris-HCl or NaH_2PO_4 (Fig. S1). For all viruses, pH 9 had no significant effect on the infectivity (Fig. 2 e-h). PANV1, PANV2, and OANV2 were also stable at pH 5. OANV1 preserved the titer at pH 5 after 1 h incubation, but dropped 10-fold after 5 h. At pH 3, all virus titers dropped significantly (PANV2 <1%; others $<1\times10^4$ PFU/ml).

Antarctic sea ice phages adsorb to their hosts effectively

All viruses were effectively adsorbed to their hosts, achieving at least ~50% binding efficiency within 6 h at 4 °C (Fig. 3). During the experimental set-up, viruses were not inactivated, since no general decrease in virus plaque numbers was observed in virus control samples. PANV2 and OANV2 showed the fastest and the most efficient adsorption, having ~80% particles adsorbed by 30 min and 1 h post infection (p.i.), respectively, and reaching ~100% binding later (Fig. 3). Adsorption rate constants k calculated for the first 30 min p.i. (n=3) were 3.9×10^{-9} and 9.0×10^{-12} ml/min for PANV2

and OANV2, respectively. PANV1 and OANV1 adsorbed with the rates of 5.4×10^{-10} and 4.6×10^{-13} ml/min, respectively, reaching ~70% adsorption by 12 h p.i.

Infection cycles of Antarctic sea ice phages result in cell lysis or host growth retardation

IceBac 372, 419, and 430 grew to early stationary stage in 4-7 days (from OD_{550}=0.2 to 1.4-1.6), showing typical growth curves of a bacterial culture. The cultures were infected at the logarithmic growth phase (*Paraglaciecola* IceBac 372: OD_{550}=0.8, ~2×10^7 CFU/ml; *Octadecabacter* IceBac 419 and 430: OD_{550}=0.6, ~3×10^9 CFU/ml) using a MOI of 8-10 to analyze one-step growth of the phages (Fig. 4). Uninfected cultures reached OD_{550}=1.6-1.7 by 124 h p.i. (Fig. 4). The turbidities of cultures infected with PANV1, PANV2, or OANV2 started to decrease at 12-20 h p.i, and eventually dropped to 0.2-0.4, indicating cell lysis (Fig. 4 a, b, d). The turbidity of OANV1-infected culture stayed at the same level as at the time of infection, showing growth retardation (Fig. 4c). For PANV1 and PANV2, an increase in the numbers of free viruses was detected at 24 h p.i., suggesting progeny virus production. The lysate titers were ~1.6×10^{10} and ~2.4×10^{11} PFU/ml for PANV1 and PANV2, respectively. In OANV1 and OANV2 infections, the increase of free viruses could not be detected with the methods used here. However, for OANV1, the number of viable *Octadecabacter* IceBac 419 cells at the time of infection (~1.1×10^9 CFU/ml) reduced almost two orders of magnitude as a result of virus addition (~2.3×10^7 CFU/ml) by 124 h p.i., while the number of viable cells in the uninfected culture of IceBac 419 was growing (~3.3×10^9 CFU/ml by 124 h). This can be interpreted as lysis caused by the virus infection. Similarly, the numbers of viable cells in the OANV2-infected IceBac 430 culture dropped noticeably (from ~1.4×10^9 at 0 h p.i. to ~5×10^6 CFU/ml at 124 h p.i.) compared to the uninfected culture (~3.5×10^9 CFU/ml at 124 h p.i.).

OANV1 is a podovirus

Based on the sequence information (see below), we re-analyzed the OANV1 virus morphology. Transmission electron micrographs of purified OANV1 particles displayed a podovirus-like morphotype: tailed virions with icosahedral heads (diameter ~68 nm, n=44) and short non-contractile tails (length ~11 nm, n= 25) (Figs. S2a and S2b). Electron micrographs were taken from two independently purified virus samples (specific infectivity 6.1×10^{13} and 3.7×10^{13} PFU/mg of protein) using two negative stains, all demonstrating consistent particle morphology. The protein patterns of the purified OANV1 particle samples were identical to each other (Fig. S2c) and similar to that previously reported (34). The particle morphology information (Figs. S2a and S2b) replaces the previously published data on OANV1, which was initially identified as a siphovirus (long flexible tail) (34).

Antarctic sea ice phages have largely unique genomes

PANV1, PANV2, OANV1, and OANV2 genomes are dsDNA molecules ranging from ~36 to ~151 kb, with GC content of 37.7-62.1 % and 61-243 predicted protein-coding ORFs (Table 1, Fig. 5a, Tables S1-4). Only PANV1 contains predicted tRNA genes (Table 1). All four virus genomes include ORFs encoding small and large terminase subunits, which are hallmark genes for tailed dsDNA bacteriophages that package their genomes into a preformed procapsid (47). ORF numbering in four genome sequences studied here was started with the ORF for the small terminase subunit (ORF1).

The overall nucleotide identity between four genomes is the lowest (~24%) between PANV1 and PANV2 and the highest (~52%) between OANV1 and OANV2. When the complete sequences were used as queries in blastn searches (somewhat similar sequences option, dated 19.02.2021) against all virus sequences (NCBI Taxonomy ID10239) in a nr nucleotide collection, typically only less than 3% of the whole sequences could be aligned with other virus sequences available, highlighting the overall uniqueness of these Antarctic sea ice virus isolates. One exception was the match of the OANV2 genome to the uncultured *Caudovirales* phage genome assembly (Genbank accession number LR798304), obtained from metagenomes from the Římov reservoir (freshwater man-made pond), Czech Republic (48): the overall identity between the genomes was 52.2% (Fig. S3a). Nonetheless, the majority of predicted ORF products (63-71%) could not be assigned with any functions, including unique sequences (43-48%) that had no homologues in the NCBI nr protein database (Fig. 5b). Surprisingly, the ratio between unique ORF products and those that had some homologous sequences in the database was about the same for all four viruses, regardless of the genome length (Fig. 5b).

About 29-37 % of the sequences had homologs in the database, allowing us to predict their functions. Blast matches revealed mosaic similarities to the sequences of other phages, as well as moderate and psychrophilic bacteria. The following functional categories were assigned to the gene products (gp): (i) proteins involved in DNA replication, recombination, modification, and metabolism; (ii) transcription and translation regulation proteins; (iii) virion and tail structural components; (iv) cell lysis; and (v) other functions (Tables S1-S4, Fig. 5). Some putative proteins could be classified to more than one category.

PANV2 gp55 has significant blast hits to phage regulatory Rha proteins, encoded by temperate phages (49, 50). Unlike the other three viruses, no lysis genes were predicted in PANV2. In OANV1, gp15 and gp16 are putatively lysis-related proteins. Noticeably, gp16 is the longest predicted OANV1 protein (2 986 residues) and it is similar to Bordetella phage BPP-1 bbp10, which is a lysin containing beta/gamma crystalline motif (blastp search 19.02.21: 50% cover, 30% identity, E-value: 3e-128). In PANV1, gp232 and gp233 were annotated as baseplate subunits having lysozyme activity, being similar to the gene products in T4-like phages (T4 gp5 and gp 25, respectively) (51, 52). In OANV2, gp19 is presumably a cell wall hydrolyze and gp29 is a lysozyme.

In addition to the categories typical for dsDNA phage genomes, additional functions were also predicted. PANV1 gp36 was predicted to be a phospholipase (HHpred search: hit 1LWB_A, probability 98.8, E-value 2e-8, 19.2.2021), thus possibly involved in lipid metabolism. PANV1 gp37 putatively belongs to the NADAR (NAD and ADP-ribose) superfamily, having hydrolyse activity and taking part in carbohydrate derivative metabolic processes (HHpred search: hit 2B3W_A, probability 100, E-value 7.1e-34, 19.02.2021). PANV1 gp51 had matches to mechanosensitive channel proteins, involved in transmembrane transport (e.g., HHpred hit to 6RLD_D, probability 99.7, E-value 7.2e-17, 19.02.2021). However, a transmembrane helix was predicted in this protein with only ~0.6 posterior probability by TMHMM v 2.0. PANV2 gp30 is a putative transpeptidase, involved in peptidoglycan cross-linking (HHpred, 4LPQ_A, probability 96.6, E-value 0.01, 19.02.2021).

Based on Virfam analysis of the neck module and part of the head and tail proteins (42), PANV1 was assigned to the category of "*Myoviridae* of Type 2", adopting the structural organization of the

myophage T4 neck. PANV2 was assigned to "*Siphoviridae* of Type 1 cluster 5", adopting the structural organization of the siphophage SPP1 neck. Both OANV1 and OANV2 were predicted to belong to "*Podoviridae* of Type 3", adopting the structural organization of the podophage P22 neck. (42). The Virfam-based classification is consistent with the tail morphology determined by transmission electron microscopy previously for PANV1, PANV2, and OANV2 (34) and here for OANV1.

Viruses related to the Antarctic sea ice phages are found in Antarctica and in other distant marine environments

The blastn search with PANV1, PANV2, OANV1, and OANV2 whole genomes as queries against IMG/VR database resulted in many hits to sequences obtained from various locations and environments. Both regions containing ORFs with assigned functions and unknown ones recruited hits. Most blastn hits covered relatively short regions (38-3870 nt), hence, to find similar viral genomes rather than separate ORFs, scaffolds with at least three regions of similarity were selected for further analysis (Table S5). While PANV1 had no such related scaffolds, the other three virus genome sequences recruited several scaffolds originating from Antarctica and other environments (Fig. 6). Notably, some of the selected scaffolds represented identical parts of each other and originated from the same project and sampling location, so likely represented sequencing of the same virus across multiple samples (the duplicates excluded in Fig. 6).

PANV2 was similar to the scaffolds assembled from saline water microbial communities from Ace Lake, Antarctica (53), and more unexpectedly, one scaffold from marine sediment microbial communities from methane seeps sampled in Hudson Canyon, US Atlantic Margin. Moreover, OANV1 was related to scaffolds from oil polluted marine microbial communities from Coal Oil Point, Santa Barbara, California, USA (54), and aqueous microbial communities from the Delaware River and Bay under freshwater to marine salinity gradient, but no samples from Antarctica (Fig. 6). On the contrary, OANV2 was similar only to scaffolds originating from saline lake microbial communities from various locations in Antarctica: Organic lake, Club lake, Deep lake, saline lake on Rauer Islands, as well as marine microbial communities from Ellis Fjord, Antarctic Ocean (53, 55). Similarity regions are distributed along the whole virus genomes and include ORFs assigned with different functions, including those encoding capsid structural proteins (Figs. S3b, S4, S5). The overall nucleotide identity between the query genomes and scaffolds retrieved from the database was ~40% for those sequences that have similar length (Table S5).

Discussion

The effect of elevated temperature, low ionic strength and acidic/alkaline conditions on viral infectivity

Although all studied phages infect their hosts at 0 °C and 4-5 °C, but not 10 °C (34), they tolerated one-hour exposures to at least 30 °C or even 50 °C (Fig. 1). Similar physical stability of virions has been observed in the tailed dsDNA phages isolated from Baltic sea ice on *Shewanella* or *Flavobacterium* (34). However, the cold-active tailed dsDNA phage 9A of *Colwellia psychrerythraea* from Arctic nepheloid layer is rapidly inactivated at 25-32.5 °C with no effect of salinity or clay particles on thermal lability (56). Cold-active tailed bacteriophages isolated from Napahai wetland and Mingyong glacier, China, typically tolerate 1 h incubations at up to 40 °C, but have varying pH

sensitivity (57-61). The sea ice viruses studied here demonstrated no infectivity losses in the absence of NaCl, which is the main salt in marine water. Moreover, PANV1 and PANV2 infectivity was not affected by the absence of Mg ions either. Such outstanding tolerance to the absence of salts as well as a wide pH tolerance must be beneficial for their survival in sea ice brine channels where salinity and pH may change across the brine network (6, 8). Some bacteriophages isolated from solar salterns, where salinity may considerably change following evaporation and rainfall events, also have wide salinity tolerance ranges (62, 63), while others may be more sensitive to lowered salinity (64).

Various patterns of sensitivity to changing environmental conditions have been observed in bacteriophages, not depending on virus morphotype or taxonomic assignments (65). Virus thermal inactivation may be caused by the release of genetic material from the capsid, as well as DNA and protein denaturation (66). Bacteriophages may aggregate at pH levels lower than their isoelectric point (67) or in lowered ionic strength conditions (68). The observed stability of PANV2 infectivity makes it an attractive model for future studies of molecular adaptation and virion architecture of viruses residing in sea ice.

Adsorption and infection cycle patterns

Viruses isolated from Arctic, Baltic and Antarctic sea ice so far seem to be very host-specific and have different temperature limits for successful host infection, being generally more psychrophilic than their host bacteria (32-34). The fast adsorption of PANV2 (90% in 30 min) and slower adsorption of PANV1 (maximally ~70% in 12 h) resulted in non-synchronized lysis and active virus production in *Paraglaciecola* observed at 24 h p.i. Putative tail fiber proteins PANV1 gp173 and PANV2 gp24 may have roles in the attachment to host cells. The similarity of the myovirus PANV1 gp232 and gp233 to lysozymes in T4-like phages suggests similar lysis mechanisms (51, 52), whereas siphovirus PANV2 may use some unknown lysis mechanisms, since no lysis-related proteins were identified. Noticeably, PANV2 gp55 is related to Rha regulatory proteins found in lambdoid phages and bacterial prophage regions (49, 50). Phages can change their state of infection as environmental conditions or the physiological condition of the host change, but whether PANV2 may establish lysogenic infection cycle remains to be clarified. Lysogeny seems to be prevalent in polar regions (29) with observed seasonal patterns (29, 69, 70).

For *Octadecabacter* podoviruses, OANV2 adsorption was faster and more efficient than that of OANV1 to their respective host strains. OANV1 gp17 and OANV2 gp10 and gp18 are putative tail spike proteins, thus possibly involved in the attachment to host cells. OANV2 infection resulted in a sharp cell density decrease at 12 h p.i., while only host growth retardation was observed for OANV1 infected culture. Nonetheless, the number of viable cells decreased during both infections, suggesting cell lysis. This is supported by the presence of putative lysis-related genes in OANV1 and OANV2 genomes.

Adsorption rate constants of four Antarctic sea ice viruses varied noticeably from the fast binder PANV2 to the slow binder OANV1 with PANV1 adsorption rate of 5.4×10^{-10} ml/min being the most similar to that observed previously in *Shewanella* phages isolated from Baltic sea ice, 1/4 and 3/49, at 4 °C (71). Infection cycles of the phages 1/4 and 3/49 were, however, considerably faster (measured at 15 °C) (71). Cold-active tailed bacteriophages from Napahai wetland and Mingyong glacier, China, have optimal plaque formation at 15-20 °C, rapid and efficient adsorption, short latent period, as well as fast and complete lysis (57-61). Thus, Antarctic sea ice phages studied here have effective, but

relatively slow infections, which may be an adaptation to slow host growth rates and preferred low temperatures (34). Similarly, slow infections with long latent periods have been determined for the *Pseudoalteromonas* phage from the North Water, Arctic, (15 h at 0 °C) (72) and *Pseudomonas putrefaciens* phage 27 from Boston harbour water (8.5 and 14 h at 2 °C on strains P10 and P19X, respectively) (73). In case of psychrophilic bacteriophage 9A infection in *Colwellia psychrerythraea* 34H, the latent period was shown to differ depending on the growth temperatures, ranging from 2.5-3 h at 8 °C to 5-10 days at -10 to -12 °C (74). Phage adsorption rates and latent period length may also depend on the host pre-incubation temperature (73, 75).

Unique genetic diversity

Viral diversity seems to be unique for Antarctica, but generally lower than that in lower-latitude marine systems (76). Overall, Antarctic phages studied here are genetically diverse and not closely related one to another or to any other sequenced sea ice phage isolates (32, 71, 77). Detected genetic similarities are rather mosaic with no clear ecological specificity. The identified functional categories are typical for tailed dsDNA phages. We suggest placing four studied viruses in the class *Caudoviricetes*. A few PANV1 proteins may take part in lipid and carbohydrate metabolism and membrane transport, thus possibly being auxiliary metabolic genes, which is commonly seen in marine phages (78). High percentage of unique sequences in Antarctic sea ice viruses emphasizes that genetic diversity of sea ice viruses remains largely unexplored. Similarly, ocean viromes contain high number of sequences having no homologs in reference databases (79).

Antarctic sea ice virus sequences have different distribution patterns on a global scale

In addition to just a handful of sea ice virus isolates with sequenced genomes, metagenomics-based studies addressing viral diversity in the Southern Ocean are also still scarce (29, 76). The structural proteins of six Baltic sea ice phages recruited translated reads from metagenomic assemblies obtained from various aquatic environments, not being restricted to the Baltic sea region (71). Here, we have given a priority to the search based on the whole genome sequences to ensure more specific hits and the possibility to easily select matches with several regions of similarity. Exploring the IMG/VR database with four Antarctic sea ice virus sequences as queries showed that they have very different distribution across environments. While PANV1-like sequences seem to be restricted to the Antarctic sea ice, OANV2-related sequences were found across various saline and marine locations around Antarctica. In addition to Antarctica samplings, PANV2 is related to the viral sequence obtained from deep-sea methane seep, while OANV1 relatives were found only in aquatic environments geographically distant from Antarctica. Obviously, ice melting may increase the transmission of viruses from Antarctica, e.g., from ancient glacial lakes, to sea ice and seawater. It is, thus, intriguing to see whether future samplings performed in Antarctica and beyond would shed light on the global distribution of viruses related to the Antarctic sea ice phages studied here.

Acknowledgements

Authors sincerely thank Sari Korhonen, Roselia Henriksson, and Heli Marttila for skillful technical assistance. Dr. Ilona Rissanen is acknowledged for her advice in negative staining. We acknowledge Electron Microscopy Unit (EMBI) and DNA Genomics and Sequencing core facility, Helsinki Institute of Life Science, University of Helsinki. The facilities and expertise of the HiLIFE

Biocomplex unit at the University of Helsinki, a member of Instruct-ERIC Centre Finland, FINStruct, and Biocenter Finland are gratefully acknowledged. We thank the Nessling Foundation (T.D.), the Kone Foundation (T.D.), and the Academy of Finland (grant 330977 to T.D.). The work conducted by the U.S. Department of Energy Joint Genome Institute (S.R.) is supported by the Office of Science of the U.S. Department of Energy under contract no. DE-AC02-05CH11231.

Competing interests

Authors declare no competing financial interests in relation to the work described.

References

1. Vancoppenolle M, Meiners KM, Michel C, Bopp L, Brabant F, Carnat G, et al. Role of sea ice in global biogeochemical cycles: emerging views and challenges. Quaternary science reviews. 2013;79:207-30.

2. Dieckmann GS, Hellmer HH. The importance of sea ice: an overview. Sea ice. 2010;2:1-22.

3. Arrigo KR. Sea ice ecosystems. Annual review of marine science. 2014;6:439-67.

4. Boetius A, Anesio AM, Deming JW, Mikucki JA, Rapp JZ. Microbial ecology of the cryosphere: sea ice and glacial habitats. Nature Reviews Microbiology. 2015;13(11):677-90.

5. Ewert M, Deming JW. Sea ice microorganisms: Environmental constraints and extracellular responses. Biology. 2013;2(2):603-28.

6. Maccario L, Sanguino L, Vogel TM, Larose C. Snow and ice ecosystems: not so extreme. Research in microbiology. 2015;166(10):782-95.

7. Thomas D, Dieckmann G. Antarctic sea ice - a habitat for extremophiles. Science. 2002;295(5555):641-4.

8. Mock T, Thomas DN. Recent advances in sea-ice microbiology. Environmental Microbiology. 2005;7(5):605-19.

9. Eicken H, Bock C, Wittig R, Miller H, Poertner H-O. Magnetic resonance imaging of sea-ice pore fluids: methods and thermal evolution of pore microstructure. Cold Regions Science and Technology. 2000;31(3):207-25.

10. Tison JL, Schwegmann S, Dieckmann G, Rintala JM, Meyer H, Moreau S, et al. Biogeochemical impact of snow cover and cyclonic intrusions on the winter Weddell Sea ice pack. Journal of Geophysical Research: Oceans. 2017;122(12):9548-71.

11. Grossi SM, Kottmeier ST, Sullivan C. Sea ice microbial communities. III. Seasonal abundance of microalgae and associated bacteria, McMurdo Sound, Antarctica. Microbial ecology. 1984;10(3):231-42.

12. Kaartokallio H. Food web components, and physical and chemical properties of Baltic Sea ice. Marine Ecology Progress Series. 2004;273:49-63.

13. Piiparinen J, Kuosa H, Rintala J-M. Winter-time ecology in the Bothnian Bay, Baltic Sea: nutrients and algae in fast ice. Polar biology. 2010;33(11):1445-61.

14. Fogwill C, Phipps S, Turney C, Golledge N. Sensitivity of the Southern Ocean to enhanced regional Antarctic ice sheet meltwater input. Earth's Future. 2015;3(10):317-29.

15. Parkinson CL, Cavalieri DJ. Antarctic sea ice variability and trends, 1979–2010. The Cryosphere. 2012;6(4):871-80.

16. Bronselaer B, Winton M, Griffies SM, Hurlin WJ, Rodgers KB, Sergienko OV, et al. Change in future climate due to Antarctic meltwater. Nature. 2018;564(7734):53-8.

17. Haumann FA, Gruber N, Münnich M, Frenger I, Kern S. Sea-ice transport driving Southern Ocean salinity and its recent trends. Nature. 2016;537(7618):89-92.

18. Maas EW, Law CS, Hall JA, Pickmere S, Currie KI, Chang F, et al. Effect of ocean acidification on bacterial abundance, activity and diversity in the Ross Sea, Antarctica. Aquatic Microbial Ecology. 2013;70(1):1-15.

19. Chénard C, Lauro FM. Exploring the viral ecology of high latitude aquatic systems. Microbial Ecology of Extreme Environments: Springer; 2017. p. 185-200.

20. López-Bueno A, Tamames J, Velázquez D, Moya A, Quesada A, Alcamí A. High diversity of the viral community from an Antarctic lake. Science. 2009;326(5954):858-61.

21. Cavicchioli R. Microbial ecology of Antarctic aquatic systems. Nature Reviews Microbiology. 2015;13(11):691-706.

22. Maranger R, Bird DF, Juniper SK. Viral and bacterial dynamics in Arctic sea ice during the spring algal bloom near Resolute, NWT, Canada. Marine Ecology Progress Series. 1994:121-7.

23. Gowing MM, Riggs BE, Garrison DL, Gibson AH, Jeffries MO. Large viruses in Ross Sea late autumn pack ice habitats. Marine Ecology Progress Series. 2002;241:1-11.

24. Gowing M. Large viruses and infected microeukaryotes in Ross Sea summer pack ice habitats. Marine Biology. 2003;142(5):1029-40.

25. Gowing MM, Garrison DL, Gibson AH, Krupp JM, Jeffries MO, Fritsen CH. Bacterial and viral abundance in Ross Sea summer pack ice communities. Marine Ecology Progress Series. 2004;279:3-12.

26. Marchant H, Davidson A, Wright S, Glazebrook J. The distribution and abundance of viruses in the Southern Ocean during spring. Antarctic Science. 2000;12(4):414-7.

27. Wells LE, Deming JW. Modelled and measured dynamics of viruses in Arctic winter sea-ice brines. Environmental Microbiology. 2006;8(6):1115-21.

28. Säwström C, Lisle J, Anesio AM, Priscu JC, Laybourn-Parry J. Bacteriophage in polar inland waters. Extremophiles. 2008;12(2):167-75.

29. Brum JR, Hurwitz BL, Schofield O, Ducklow HW, Sullivan MB. Seasonal time bombs: dominant temperate viruses affect Southern Ocean microbial dynamics. The ISME journal. 2016;10(2):437-49.

30. Anesio AM, Bellas CM. Are low temperature habitats hot spots of microbial evolution driven by viruses? Trends in microbiology. 2011;19(2):52-7.

31. Yu Z-C, Chen X-L, Shen Q-T, Zhao D-L, Tang B-L, Su H-N, et al. Filamentous phages prevalent in *Pseudoalteromonas* spp. confer properties advantageous to host survival in Arctic sea ice. The ISME journal. 2015;9(4):871-81.

32. Borriss M, Helmke E, Hanschke R, Schweder T. Isolation and characterization of marine psychrophilic phage-host systems from Arctic sea ice. Extremophiles. 2003;7(5):377-84.

33. Luhtanen A-M, Eronen-Rasimus E, Kaartokallio H, Rintala J-M, Autio R, Roine E. Isolation and characterization of phage–host systems from the Baltic Sea ice. Extremophiles. 2014;18(1):121-30.

34. Luhtanen A-M, Eronen-Rasimus E, Oksanen HM, Tison J-L, Delille B, Dieckmann GS, et al. The first known virus isolates from Antarctic sea ice have complex infection patterns. FEMS microbiology ecology. 2018;94(4):fiy028.

35. Adams MH. Bacteriophages: Citeseer; 1959.

36. Schneider CA, Rasband WS, Eliceiri KW. NIH Image to ImageJ: 25 years of image analysis. Nature methods. 2012;9(7):671-5.

37. Bankevich A, Nurk S, Antipov D, Gurevich AA, Dvorkin M, Kulikov AS, et al. SPAdes: a new genome assembly algorithm and its applications to single-cell sequencing. Journal of computational biology. 2012;19(5):455-77.

38. Madeira F, Park YM, Lee J, Buso N, Gur T, Madhusoodanan N, et al. The EMBL-EBI search and sequence analysis tools APIs in 2019. Nucleic acids research. 2019;47(W1):W636-W41.

39. Altschul SF, Gish W, Miller W, Myers EW, Lipman DJ. Basic local alignment search tool. Journal of molecular biology. 1990;215(3):403-10.

40. Lu S, Wang J, Chitsaz F, Derbyshire MK, Geer RC, Gonzales NR, et al. CDD/SPARCLE: the conserved domain database in 2020. Nucleic acids research. 2020;48(D1):D265-D8.

41. Zimmermann L, Stephens A, Nam S-Z, Rau D, Kübler J, Lozajic M, et al. A completely reimplemented MPI bioinformatics toolkit with a new HHpred server at its core. Journal of molecular biology. 2018;430(15):2237-43.

42. Lopes A, Tavares P, Petit M-A, Guérois R, Zinn-Justin S. Automated classification of tailed bacteriophages according to their neck organization. BMC genomics. 2014;15(1):1-17.

43. Chan PP, Lowe TM. tRNAscan-SE: searching for tRNA genes in genomic sequences. Gene Prediction: Springer; 2019. p. 1-14.

44. Roux S, Páez-Espino D, Chen I-MA, Palaniappan K, Ratner A, Chu K, et al. IMG/VR v3: an integrated ecological and evolutionary framework for interrogating genomes of uncultivated viruses. Nucleic Acids Research. 2021;49(D1):D764-D75.

45. Darzentas N. Circoletto: visualizing sequence similarity with Circos. Bioinformatics. 2010;26(20).

46. Sullivan MJ, Petty NK, Beatson SA. Easyfig: a genome comparison visualizer. Bioinformatics. 2011;27(7):1009-10.

47. Adriaenssens EM, Cowan DA. Using signature genes as tools to assess environmental viral ecology and diversity. Applied and environmental microbiology. 2014;80(15):4470-80.

48. Kavagutti VS, Andrei A-Ş, Mehrshad M, Salcher MM, Ghai R. Phage-centric ecological interactions in aquatic ecosystems revealed through ultra-deep metagenomics. Microbiome. 2019;7(1):1-15.

49. Henthorn KS, Friedman DI. Identification of related genes in phages phi 80 and P22 whose products are inhibitory for phage growth in *Escherichia coli* IHF mutants. Journal of bacteriology. 1995;177(11):3185-90.

50. Casjens SR, Gilcrease EB, Winn-Stapley DA, Schicklmaier P, Schmieger H, Pedulla ML, et al. The generalized transducing Salmonella bacteriophage ES18: complete genome sequence and DNA packaging strategy. Journal of bacteriology. 2005;187(3):1091-104.

51. Szewczyk B, Bienkowska-Szewczyk K, Kozloff LM. Identification of T4 gene 25 product, a component of the tail baseplate, as a 15K lysozyme. Molecular and General Genetics MGG. 1986;202(3):363-7.

52. Petrov VM, Ratnayaka S, Nolan JM, Miller ES, Karam JD. Genomes of the T4-related bacteriophages as windows on microbial genome evolution. Virology journal. 2010;7(1):1-19.

53. Panwar P, Allen MA, Williams TJ, Hancock AM, Brazendale S, Bevington J, et al. Influence of the polar light cycle on seasonal dynamics of an Antarctic lake microbial community. Microbiome. 2020;8(1):1-24.

54. Hawley ER, Malfatti SA, Pagani I, Huntemann M, Chen A, Foster B, et al. Metagenomes from two microbial consortia associated with Santa Barbara seep oil. Marine genomics. 2014;18:97-9.

55. Tschitschko B, Erdmann S, DeMaere MZ, Roux S, Panwar P, Allen MA, et al. Genomic variation and biogeography of Antarctic haloarchaea. Microbiome. 2018;6(1):1-16.

56. Wells LE, Deming JW. Effects of temperature, salinity and clay particles on inactivation and decay of cold-active marine Bacteriophage 9A. Aquatic microbial ecology. 2006;45(1):31-9.

57. Ji X, Yu H, Zhang Q, Lin L, Wei Y. Isolation and characterization of a novel lytic cold-active bacteriophage VNPH-1 from the Napahai wetland in China. Annals of microbiology. 2015;65(3):1789-96.

58. Ji X, Zhang C, Fang Y, Zhang Q, Lin L, Tang B, et al. Isolation and characterization of glacier VMY22, a novel lytic cold-active bacteriophage of *Bacillus cereus*. Virologica Sinica. 2015;30(1):52-8.

59. Li M, Wang J, Zhang Q, Lin L, Kuang A, Materon LA, et al. Isolation and characterization of the lytic cold-active bacteriophage MYSP06 from the Mingyong glacier in China. Current microbiology. 2016;72(2):120-7.

60. Qin K, Ji X, Zhang C, Ding Y, Kuang A, Zhang S, et al. Isolation and characterization of wetland VSW-3, a novel lytic cold-active bacteriophage of *Pseudomonas fluorescens*. Canadian journal of microbiology. 2017;63(2):110-8.

61. Xiang Y, Wang S, Li J, Wei Y, Zhang Q, Lin L, et al. Isolation and characterization of two lytic cold-active bacteriophages infecting *Pseudomonas fluorescens* from the Napahai plateau wetland. Canadian journal of microbiology. 2018;64(3):183-90.

62. Kukkaro P, Bamford DH. Virus–host interactions in environments with a wide range of ionic strengths. Environmental microbiology reports. 2009;1(1):71-7.

63. Rodela ML, Sabet S, Peterson A, Dillon JG. Broad environmental tolerance for a *Salicola* host-phage pair isolated from the Cargill Solar Saltworks, Newark, CA, USA. Microorganisms. 2019;7(4):106.

64. Aalto AP, Bitto D, Ravantti JJ, Bamford DH, Huiskonen JT, Oksanen HM. Snapshot of virus evolution in hypersaline environments from the characterization of a membrane-containing Salisaeta icosahedral phage 1. Proceedings of the National Academy of Sciences. 2012;109(18):7079-84.

65. Jończyk E, Kłak M, Międzybrodzki R, Górski A. The influence of external factors on bacteriophages. Folia microbiologica. 2011;56(3):191-200.

66. Vörös Z, Csík G, Herényi L, Kellermayer M. Temperature-dependent nanomechanics and topography of bacteriophage T7. Journal of virology. 2018;92(20).

67. Langlet J, Gaboriaud F, Gantzer C. Effects of pH on plaque forming unit counts and aggregation of MS2 bacteriophage. Journal of Applied Microbiology. 2007;103(5):1632-8.

68. Szermer-Olearnik B, Drab M, Mąkosa M, Zembala M, Barbasz J, Dąbrowska K, et al. Aggregation/dispersion transitions of T4 phage triggered by environmental ion availability. Journal of nanobiotechnology. 2017;15(1):1-15.

69. Laybourn-Parry J, Marshall WA, Madan NJ. Viral dynamics and patterns of lysogeny in saline Antarctic lakes. Polar Biology. 2007;30(3):351-8.

70. Säwström C, Anesio MA, Granéli W, Laybourn-Parry J. Seasonal viral loop dynamics in two large ultraoligotrophic Antarctic freshwater lakes. Microbial ecology. 2007;53(1):1-11.

71. Senčilo A, Luhtanen AM, Saarijärvi M, Bamford DH, Roine E. Cold-active bacteriophages from the Baltic sea ice have diverse genomes and virus–host interactions. Environmental microbiology. 2015;17(10):3628-41.

72. Middelboe M, Nielsen TG, Bjørnsen PK. Viral and bacterial production in the North Water: in situ measurements, batch-culture experiments and characterization and distribution of a virus–host system. Deep Sea Research Part II: Topical Studies in Oceanography. 2002;49(22-23):5063-79.

73. Delisle A, Levin R. Effect of temperature on an obligately psychrophilic phage-host system of *Pseudomonas putrefaciens*. Antonie Van Leeuwenhoek. 1972;38(1):9-15.

74. Wells LE, Deming JW. Characterization of a cold-active bacteriophage on two psychrophilic marine hosts. Aquatic microbial ecology. 2006;45(1):15-29.

75. Sillankorva S, Oliveira R, Vieira MJ, Sutherland I, Azeredo J. Pseudomonas fluorescens infection by bacteriophage ΦS1: the influence of temperature, host growth phase and media. FEMS microbiology letters. 2004;241(1):13-20.

76. Brum JR, Ignacio-Espinoza JC, Roux S, Doulcier G, Acinas SG, Alberti A, et al. Patterns and ecological drivers of ocean viral communities. Science. 2015;348(6237).

77. Colangelo-Lillis JR, Deming JW. Genomic analysis of cold-active Colwelliaphage 9A and psychrophilic phage–host interactions. Extremophiles. 2013;17(1):99-114.

78. Brum JR, Sullivan MB. Rising to the challenge: accelerated pace of discovery transforms marine virology. Nature Reviews Microbiology. 2015;13(3):147-59.

79. Hurwitz BL, Sullivan MB. The Pacific Ocean Virome (POV): a marine viral metagenomic dataset and associated protein clusters for quantitative viral ecology. PloS one. 2013;8(2):e57355.

Tables

Table 1. Antarctic sea ice viruses used in this study.

Virus[a]	Virus morphotype, head diameter	Host strain[a]	Virus genome[b]				
			Length (bp)	GC%	ORFs	tRNAs	Genbank acc. no
Paraglaciecola Antarctic GD virus 1 (PANV1)	Icosahedral head, long contractile tail (myovirus-type), 71±7 nm[a]	*Paraglaciecola* IceBac 372	150 766	37.7	243	4	MW805361
Paraglaciecola Antarctic JLT virus 2 (PANV2)	Icosahedral head, long non-contractile tail (siphovirus-type), 52±8 nm[a]	*Paraglaciecola* IceBac 372	35 731	41.0	73	0	MW805362
Octadecabacter Antarctic BD virus 1 (OANV1)	Icosahedral head, short non-contractile tail (podovirus-type), 68 nm[b]	*Octadecabacter* IceBac 419	48 354	62.1	61	0	MW805363
Octadecabacter Antarctic DB virus 2 (OANV2)	Icosahedral head, short non-contractile tail (podovirus-type), 53±7 nm[a]	*Octadecabacter* IceBac 430	39 241	53.3	76	0	MW805364

[a] data from (34);

[b] this study.

Figures

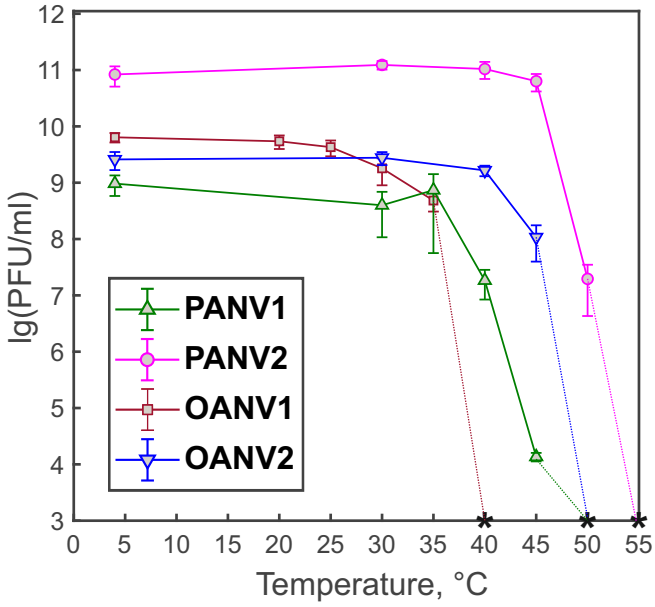

Figure 1. Stability of Antarctic sea ice virus infectivity after 1 h exposure to different temperatures. Bars represent means of at least three independent replicates with standard error of the mean. Asterisks indicate that the titers are under the detection limit ($<1\times10^3$ PFU/ml).

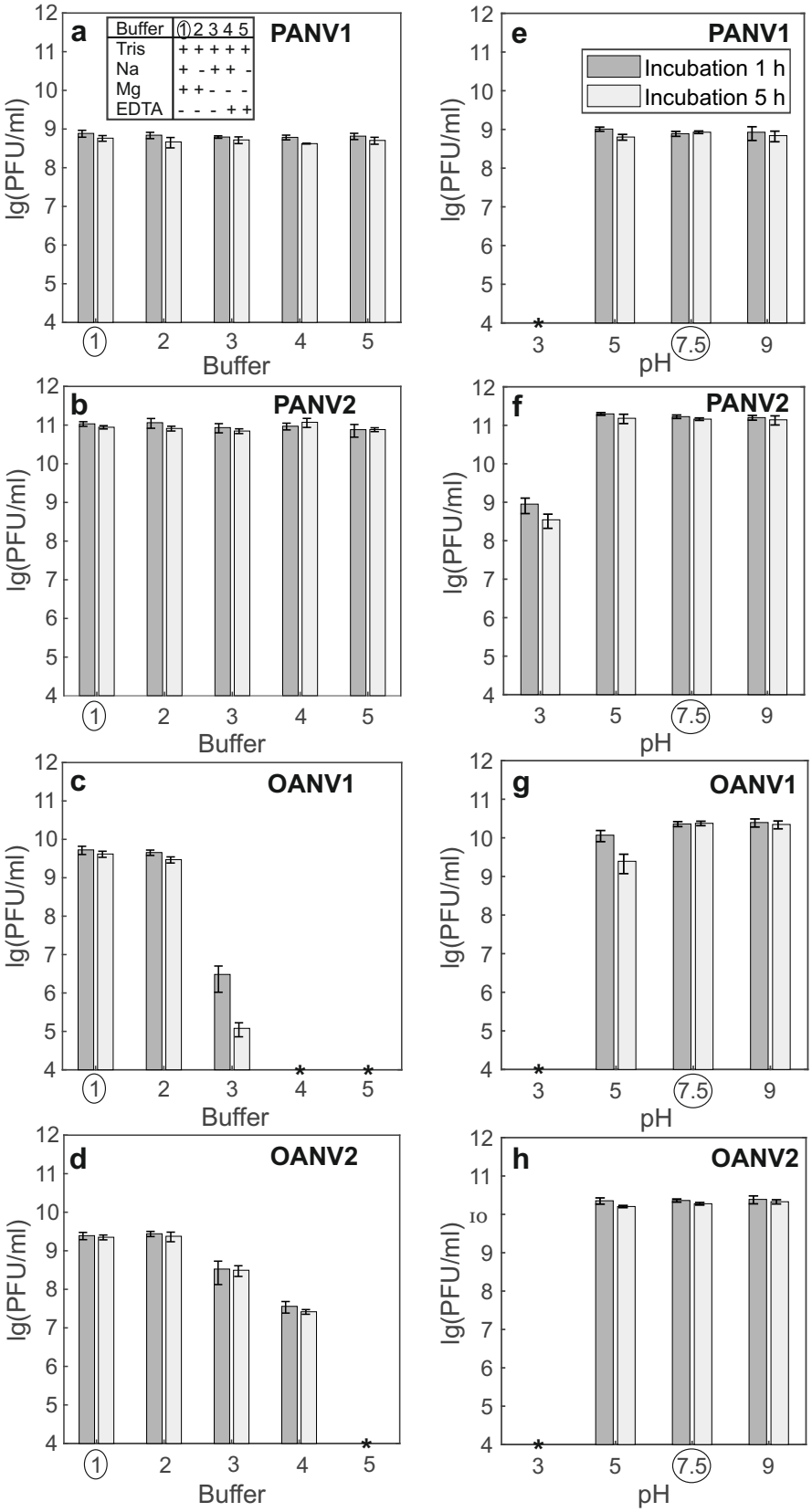

Figure 2. Stability of virus infectivity in buffers with different ion composition and pH. Virus stocks were diluted either in SM buffer (circle in all panels), (a-d) modified SM buffers where some components were omitted (key in a), or (e-h) modified SM buffers of different pH. The incubation lasted 1 h (dark grey) and 5 h (light grey). Bars represent means of at least three independent replicates with standard error of the mean. Asterisk indicates that the titer is under the detection limit ($<1\times10^4$ PFU/ml).

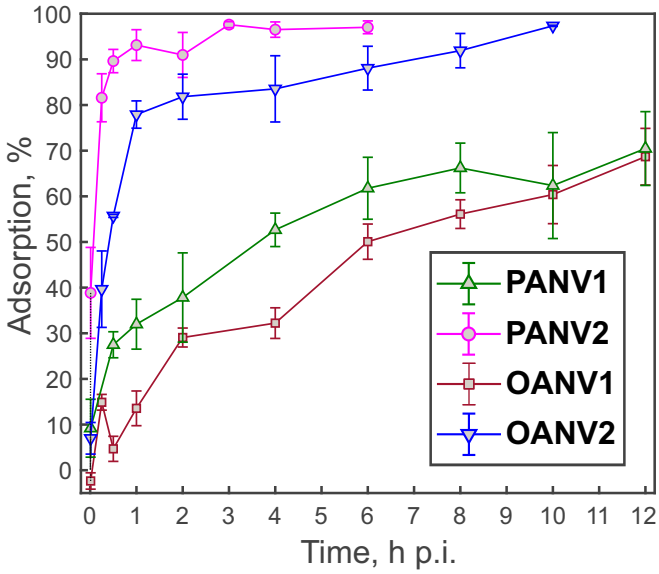

Figure 3. Adsorption efficiency shown as percentage of bound viruses at 4 °C. Means of at least three independent replicates are presented with standard error of the mean.

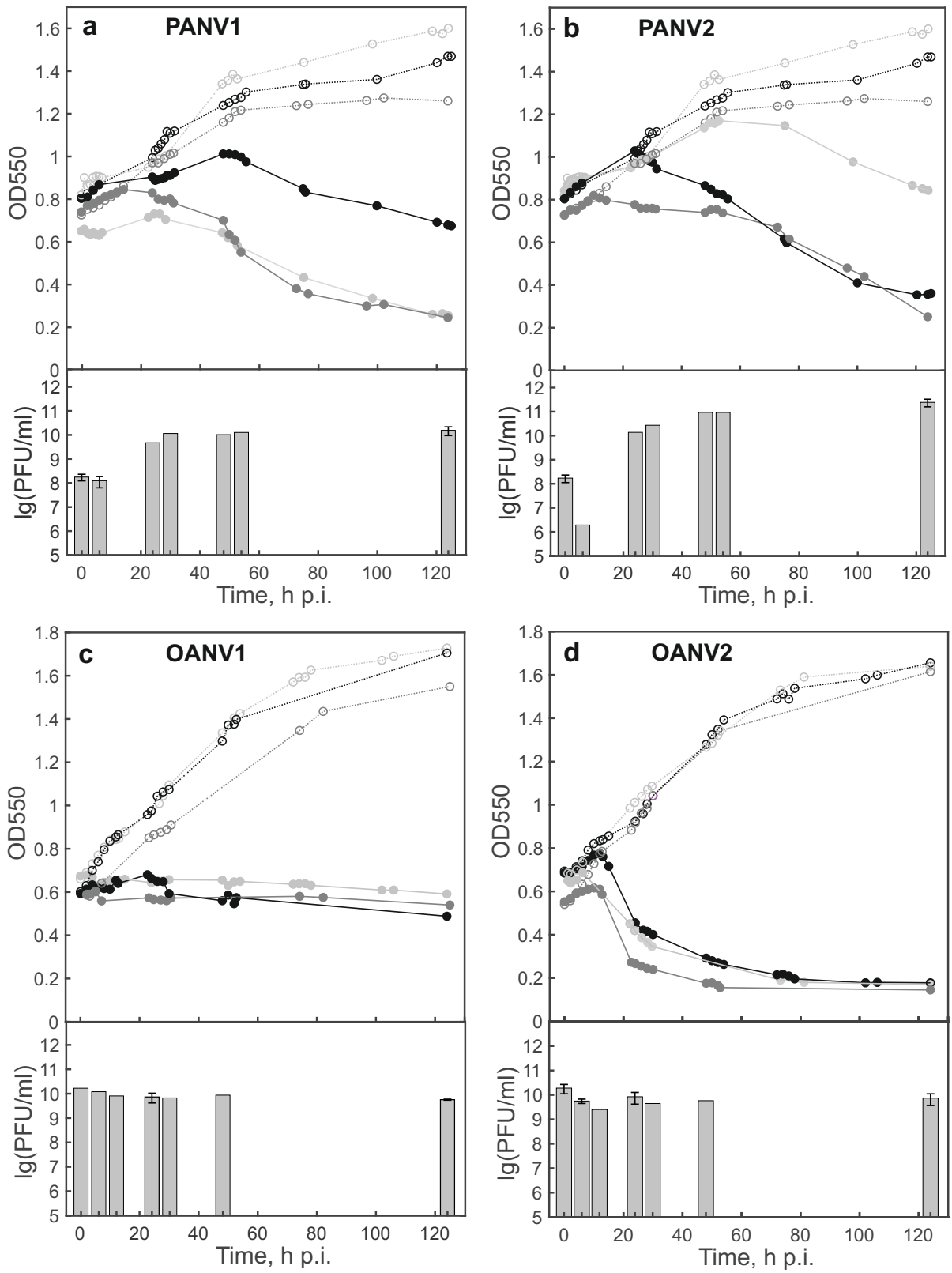

Figure 4. One-step growth curves of (a) PANV1 and (b) PANV2 in *Paraglaciecola* IceBac 372, (c) OANV1 in *Octadecabacter* IceBac 419, and (d) OANV2 in *Octadecabacter* IceBac 430. Growth curves of uninfected (open circles, dashed lines) and infected (closed circles, solid lines) cultures from three independent repeats are shown in the upper panels. Curves with same shades of grey represent the same repeat. The numbers of free viruses are shown as bars in lower panels: means with standard error of the mean where appropriate (n=3), otherwise means of n=2.

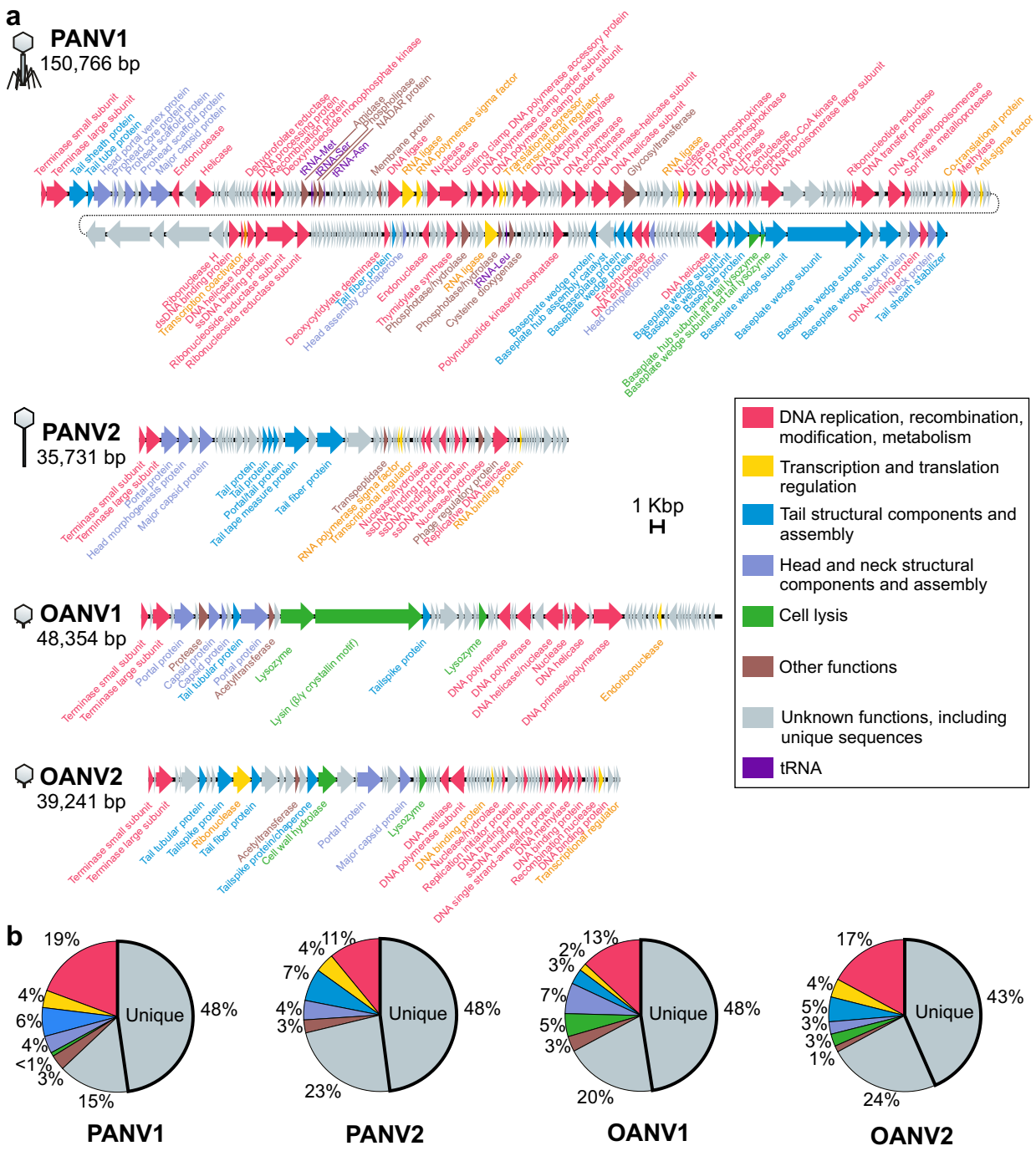

Figure 5. (a) Genomes of PANV1, PANV2, OANV1, and OANV2. ORF colors refer to the assigned functional categories (inset, same for (a) and (b)). Virus morphotypes are indicated schematically on the left. (b) Distribution of functional categories assigned to the protein-coding ORFs of PANV1, PANV2, OANV1, and OANV2. The portions of unique ORF products not having homologs in the NCBI nr protein database are outlined with bold.

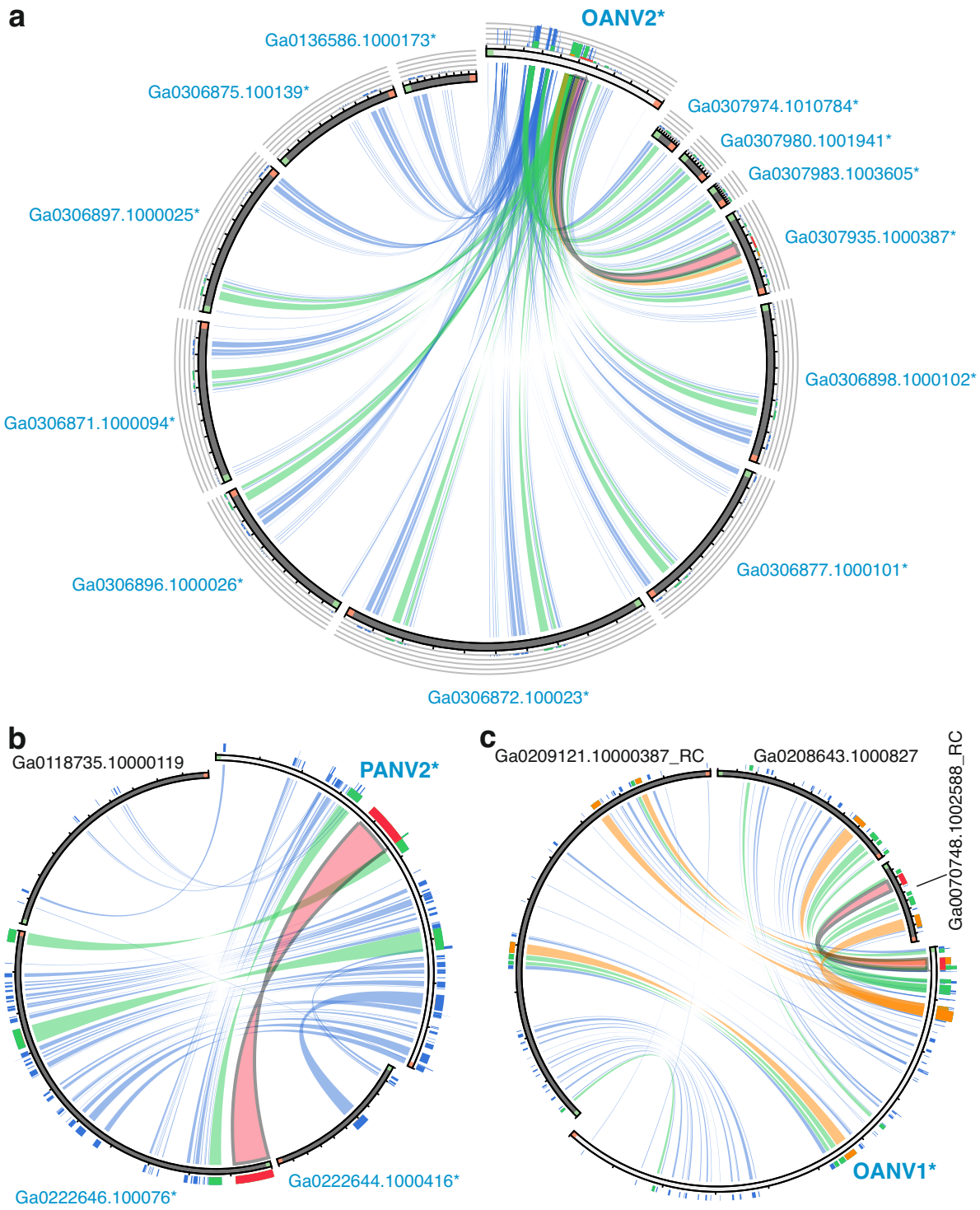

Figure 6. Visualizing sequence similarities between (a) OANV2, (b) PANV2, and (c) OANV1 and corresponding metagenome-derived scaffolds found in IMG/VR database (see Table S5). The figure was generated with Circoletto, using "score/max" ratio colouring with blue≤0.25, green≤0.50, orange≤0.75, and red>0.75. Orientation of the sequences is clockwise, in addition, sequence starts are marked with green and ends with red. Some sequences are presented as reverse complements (RC). Sequences originating from Antarctica are in blue and marked with asterisk.